Neuron
Article

Decoding Wakefulness Levels from Typical fMRI Resting-State Data Reveals Reliable Drifts between Wakefulness and Sleep

Enzo Tagliazucchi[1] and Helmut Laufs[1,2,*]
[1]Department of Neurology and Brain Imaging Center, Goethe University Frankfurt am Main, Theodor-Stern-Kai 7, 60590 Frankfurt am Main, Germany
[2]Department of Neurology, University Hospital Schleswig Holstein, Arnold-Heller-Straße 3, 24105 Kiel, Germany
*Correspondence: h.laufs@neurologie.uni-kiel.de
http://dx.doi.org/10.1016/j.neuron.2014.03.020

SUMMARY

The mining of huge databases of resting-state brain activity recordings represents state of the art in the assessment of endogenous neuronal activity—and may be a promising tool in the search for functional biomarkers. However, the resting state is an uncontrolled condition and its heterogeneity is neither sufficiently understood nor accounted for. We test the hypothesis that subjects exhibit unstable wakefulness, i.e., drift into sleep during typical resting-state experiments. Analyzing 1,147 resting-state functional magnetic resonance data sets, we revealed a reliable loss of wakefulness in a third of subjects within 3 min and demonstrated the dynamic nature of the resting state, with fundamental changes in the associated functional neuroanatomy. Implications include the necessity of wakefulness monitoring and modeling, taking measures to maintain a state of wakefulness, acknowledging the possibility of sleep and exploring its consequences, and especially the critical assessment of possible false-positive or false-negative results.

INTRODUCTION

In basic and clinical neuroscience, more and more large collaborative efforts aim at building massive databases suitable to support high impact studies of human brain function, for example the BRAIN initiative (Brain Activity Map Project) (Alivisatos et al., 2012, Devor et al., 2013). Other recent initiatives are gathering a large number of fMRI data sets and making them available to the international neuroimaging research community as a resource (for example, the 1000 Functional Connectomes Project, http://fcon_1000.projects.nitrc.org) (Biswal et al., 2010). Not driven by specific hypotheses, this data-centered approach can open exciting new avenues of discovery science of brain function—provided careful and correct execution.

While such attempts extend to all levels of brain function across different species, there is special interest in using modern neuroimaging techniques to understand the organization of neural activity in the healthy and particularly the diseased human brain (Zhang and Raichle, 2010). Technically, a paradigm-less experimental setting appears especially suitable for building multicenter databases keeping minimal any confounding influence by the local experimental settings. Biologically, resting-state studies are fascinating because of the observation that despite task absence, during the so-called resting state, brain networks can be derived that commonly engage in typical task processing (Smith et al., 2009). As we will detail below, it has been suggested and is generally accepted, that alterations in brain function cannot only be observed during task performance, i.e., while the system is "under load," but also in the absence of any externally induced task, i.e., during rest, when distributed brain regions exhibit coherent low-frequency fluctuations (with periods around 10–100 s) binding them together into identifiable functional networks (Gusnard et al., 2001; Raichle, 2006; Fox and Raichle, 2007). However, the use of these networks to categorize different cohorts—or as biomarkers for different groups—presupposes that the same resting state induces different neuronal fluctuations in different groups. Put simply, one has to assume that two groups of subjects are thinking about the same things in order to infer a neurophysiological difference. Clearly, this is a tenuous assumption. In what follows, we show that not only could subjects be thinking about different things, but they could be in completely different brain (or sleep) states.

The promising future of resting-state fMRI to study the human brain already has prompted large collaborative efforts aimed at developing biomarkers for disease and to unravel the large-scale human functional connectome (Biswal et al., 2010; The HD-200 Consortium, 2012; Di Martino et al., 2013). Resting-state fMRI studies have already been successfully used to assess the functional alterations associated with a wide spectrum of pathologies, including Alzheimer's disease (Rombouts et al., 2005; Wang et al., 2006; Sorg et al., 2007), schizophrenia (Zhou et al., 2007), autism (Di Martino et al., 2011), attention-deficit hyperactivity disorder (ADHD) (Zang et al., 2007; Uddin et al., 2008), epilepsy (Pereira et al., 2010; Luo et al., 2011), chronic pain (Baliki et al., 2008), and more (Greicius, 2008).

All of the aforementioned resting-state experiments are assumed to have been conducted during wakefulness. Wakeful rest is a fundamentally uncontrolled brain state, usually defined by a lack of sensory stimulation, motor output, and cognitive

effort. The uncontrolled nature of resting-state fMRI has caused concern due to the possibility of confounds, either physiological (fluctuations in respiration and cardiac rate [Birn et al., 2006; Shmueli et al., 2007; Birn et al., 2008; Murphy et al., 2013]) or due to subject motion (Van Dijk et al., 2012). It has also been suggested that brain activity during rest is very heterogeneous and represents a wide range of contents and cognitive states (Christoff et al., 2009; Richiardi et al., 2011). A more extreme and systematic departure from wakeful rest can simply occur if subjects fall asleep during the scanning session, entering nonrapid eye movement (NREM) sleep. This brings about major physiological changes in behavior and the underlying brain functional architecture. Its spatial and functional extent have been characterized by a number of neuroimaging studies (Maquet, 2000; Boly et al., 2012; Horovitz et al., 2009; Picchioni et al., 2013; Spoormaker et al., 2010; Sämann et al., 2011; Tagliazucchi et al., 2012a, 2012b, 2013a, 2013b). The ear plug-dampened fMRI-typical monotonous scanner acoustic noise and vibrations represent the sole sensory stimulation during resting-state experiments in the absence of any alerting task engagement. Because such monotony and absence of attention demanding stimuli promote fatigue (Richter et al., 2005; Baumann et al., 1968) and also following from own experience, we hypothesized that during a typical resting-state experiment the likelihood of subjects falling asleep is high, with potential nonnegligible consequences for the study of the functional architecture of the human brain, including the possibility of false positives or negatives when analyzing functional connectivity or network measures, as well as measures that characterize hemodynamic time series.

Here, we test our hypothesis that sleep commonly occurs during resting-state fMRI by assessing the degree of wakefulness in a cohort of 71 subjects scanned simultaneously with polysomnographic electroencephalography (EEG) and fMRI. Polysomnographic EEG is the gold standard for sleep scoring following the rules proposed by the American Academy of Sleep Medicine (AASM, 2007). Based on this data, we trained and validated a support vector machine (SVM) classifier for decoding sleep (Tagliazucchi et al., 2012a) and applied it to the 1,147 resting-state fMRI data sets of the 1000 Functional Connectomes Project (Biswal et al., 2010). Highlighting the biological relevance of our findings, we demonstrate that SVM-based sleep scoring identifies brain states exhibiting well-described sleep stage-specific hemodynamic characteristics in the resting-state activity, which were independent of the SVM training.

RESULTS

We demonstrate the prevalence of sleep in two different resting-state data sets: (1) "Frankfurt data set," EEG-fMRI of 71 subjects instructed to lie still in the scanner bore with eyes closed and scanned for 52 min with experiments starting at 7:00 p.m., and (2) a large cohort of subjects scanned by different research groups throughout the world (termed "Connectome data set").

EEG-fMRI Recordings Reveal Rapid Sleep Onset during the Resting State

The EEGs of the Frankfurt data set were sleep staged according to AASM rules classifying each 30 s epoch of the experiment as either awake or as any one of the three stages of NREM sleep: N1 (light sleep), N2, and N3 (slow wave or deep sleep). Figure 1 summarizes the results. The number of continuously awake subjects (subjects in uninterrupted wakefulness) quickly decreased after the resting-state scanning sequence started (Figure 1A)—of note, 5% of the subjects were already asleep at the time of the fMRI scan start. After 10 min had elapsed (a typical duration of a resting-state experiment), one in two subjects had undergone a transition into light sleep at least once. The probability of finding an awake subject decreased rapidly within the first 5 min of the experiment and reached a minimum ($p = 0.42$) ~20 min into the experiment before then slowly increasing again (Figure 1B). After 4 min of the experiment, one-third of the subjects were asleep, and ~50% were asleep after 10 min. Following the natural course of sleep, early in the scan, N1 sleep was predominant with a peak at ~10 min ($p \approx 0.5$). After this point, the probability of finding a subject in N2 sleep rapidly increased to a maximum at ~20 min ($p \approx 0.3$). While subjects did not reach N3 sleep during the first 15 min, this changed later in the experiment, with a peak in the N3 sleep probability at ~30 min ($p \approx 0.2$). Overall, subjects were asleep 40% of the scanning time (Figure 1C).

An fMRI-Based SVM Classifier Accurately Detects Sleep

The 55 subjects in the Frankfurt data who fell asleep during the scan were split into two groups: a training set (30 subjects) and a testing set (25 subjects). Based on AASM rules (AASM, 2007), the training set was further subdivided into wakefulness and the three NREM sleep stages. Using nonoverlapping 2 min windows, functional connectivity was computed in the training data between mean BOLD signals from all regions in the automated anatomical labeling (AAL) template (Tzourio-Mazoyer et al., 2002). Only those connections yielding significant differences between pairs of sleep stages ($p < 0.05$, Student's t test, Bonferroni corrected) were kept to train the multiclass SVM classifier. These connections are shown in Figure 2. The most remarkable feature of these patterns is the surge of increased functional connectivity during N1 and N2 sleep (compared to wakefulness) and the general connectivity breakdown observed during N3 sleep (compared to wakefulness and all other NREM sleep stages). After optimal parameter selection via 5-fold cross-validation, the performance of the classifier was evaluated in the testing data set using a 2 min sliding window to compute functional connectivity between AAL regions, obtaining an overall accuracy of 75% (given a chance accuracy of 25%).

Our data features were correlation matrices over short periods of time, pooled over both time and subjects—where each data feature was equipped with a sleep stage label, based upon EEG. We note the possible classifier outputs as SVM_i ($i = 1,2,3,4$), starting from wakefulness ($i = 1$) to N3 sleep ($i = 4$), and the AASM-scored (based on the EEG data) sleep stages as EEG_i ($i = 1,2,3,4$) (analogous enumeration). Thus, the confusion matrix $C_{i,j}$ (i.e., the matrix containing the accuracy of all pairwise classification outcomes) can be expressed as $C_{i,j} = P(SVM_i|EEG_j)$. In Figure 3A, all matrix elements of $C_{i,j}$ are plotted, showing that classification accuracy was highest for wakefulness and lowest for N1 sleep, but in

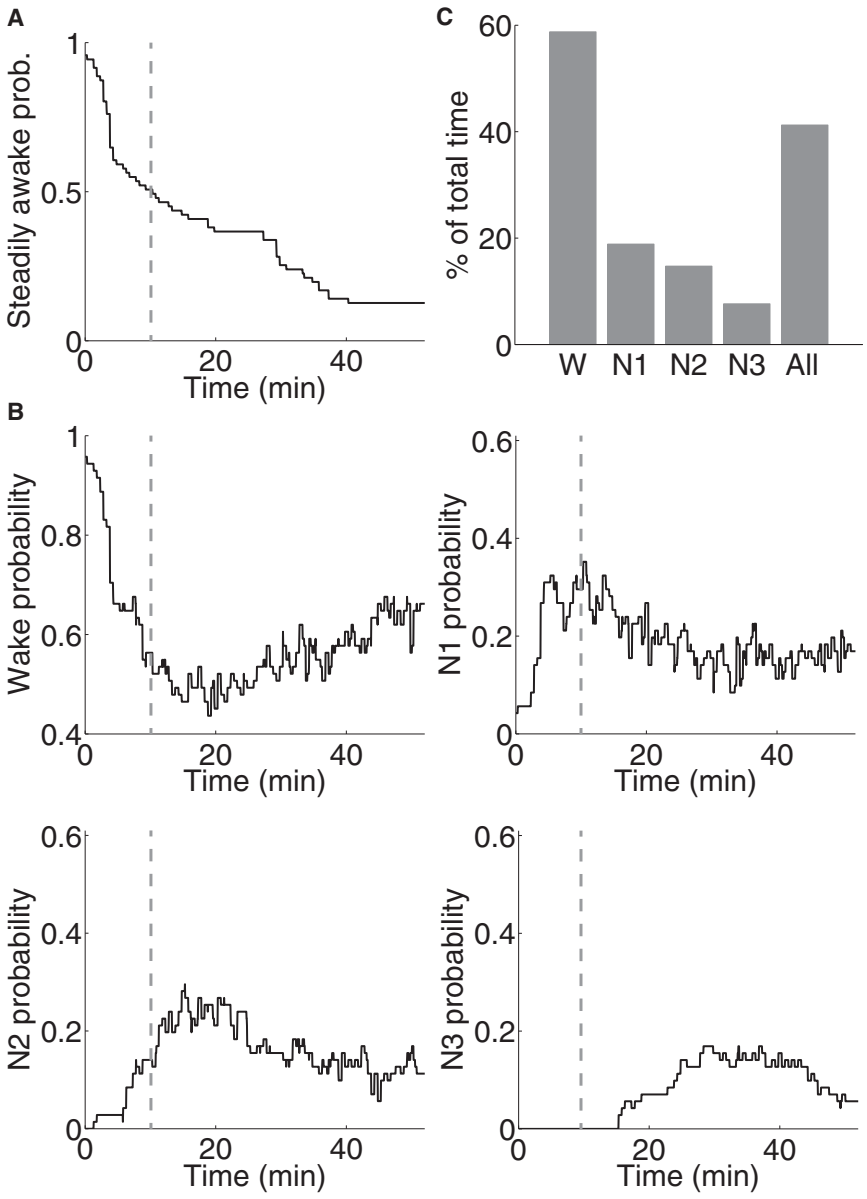

Figure 1. Subjects Quickly Fall Asleep during Resting-State fMRI Recordings

(A) Probability of subjects being continuously awake as a function of time. After 10 min, ~50% of the subjects had at least one epoch of sleep.

(B) Probability of subjects being awake and in the different NREM sleep stages (N1, N2, and N3 sleep) as a function of time.

(C) Total time spent by the subjects in wakefulness and all NREM sleep stages. Throughout ~40% of the experiment, subjects were asleep. The vertical dashed lines indicate that 10 min have elapsed since the experiment started.

all cases above the level of chance. The probability of correct detection given a certain classifier output can be obtained—via Bayes' rule—from the inverse conditional probabilities $P(EEG_i|SVM_j)$, plotted in Figure 3B. Highest confidence in the SVM classifier output corresponds to wakefulness and N3 sleep, with lower probabilities for N1 and N2 sleep. Notably, in the case of misclassifications of the SVM scoring compared to the "true" gold standard EEG scoring, the classifier was much more likely to score wakefulness in the case of "true" sleep than to classify any epoch as sleep in the case of "true" wakefulness. In other words, sleep classification in the Connectome data set was conservative, i.e., wakefulness—if at all—was overestimated. We excluded the possibility of the classifier detecting a temporal trend other than sleep depth (see Figure S6 available online).

Decoding Sleep in a Large Resting-State Data Set Revealed Regular Loss of Wakefulness

We then applied the classifier to the resting-state fMRI data of 1,147 subjects obtained from the 1000 Functional Connectomes Project (Biswal et al., 2010). Functional connectivity between all AAL regions and those corresponding to the connections presented in Figure 2 was computed based on 2 min sliding windows and served as input for the multiclass SVM classifier. Statistics summarizing the results are presented in Figure 4A and Figure 4B. The Connectome data set scanning sessions were shorter than those of the Frankfurt data set, hence, for ease of comparison, results are reported only for the first 5 min aside the results of the first 5 min of the EEG-based sleep-staged Frankfurt data set (Figure 4A). One-third of the subjects of the Connectome data set did not maintain steady wakefulness for longer than ~3 min—compared to ~4 min in the Frankfurt data set. In both data sets, the proportion of continuously awake subjects diminished over time, with a faster rate observed in the Connectome data set (8% of subjects per minute versus 15% per minute, obtained from the slope of the best linear fit during the first 5 min). Furthermore, in both data sets, the probability of finding an awake subject decreased monotonously with time, and the probability of finding a subject in N1 sleep monotonously increased with the latter being overall smaller for the Connectome data set. The probability of finding subjects in N2 sleep increased with elapsed time and was comparable for the two data sets. Finally, subjects from the Frankfurt data set did not enter N3 sleep at all within the first 5 min of the scanning session, whereas the SVM classifier detected N3 sleep in the Connectome data set. This probability did not show any monotonous trend over time and thus might have arisen from misclassifications. Finally, in both data sets wakefulness was the most prevalent sleep stage, followed by N1, N2, and N3 sleep.

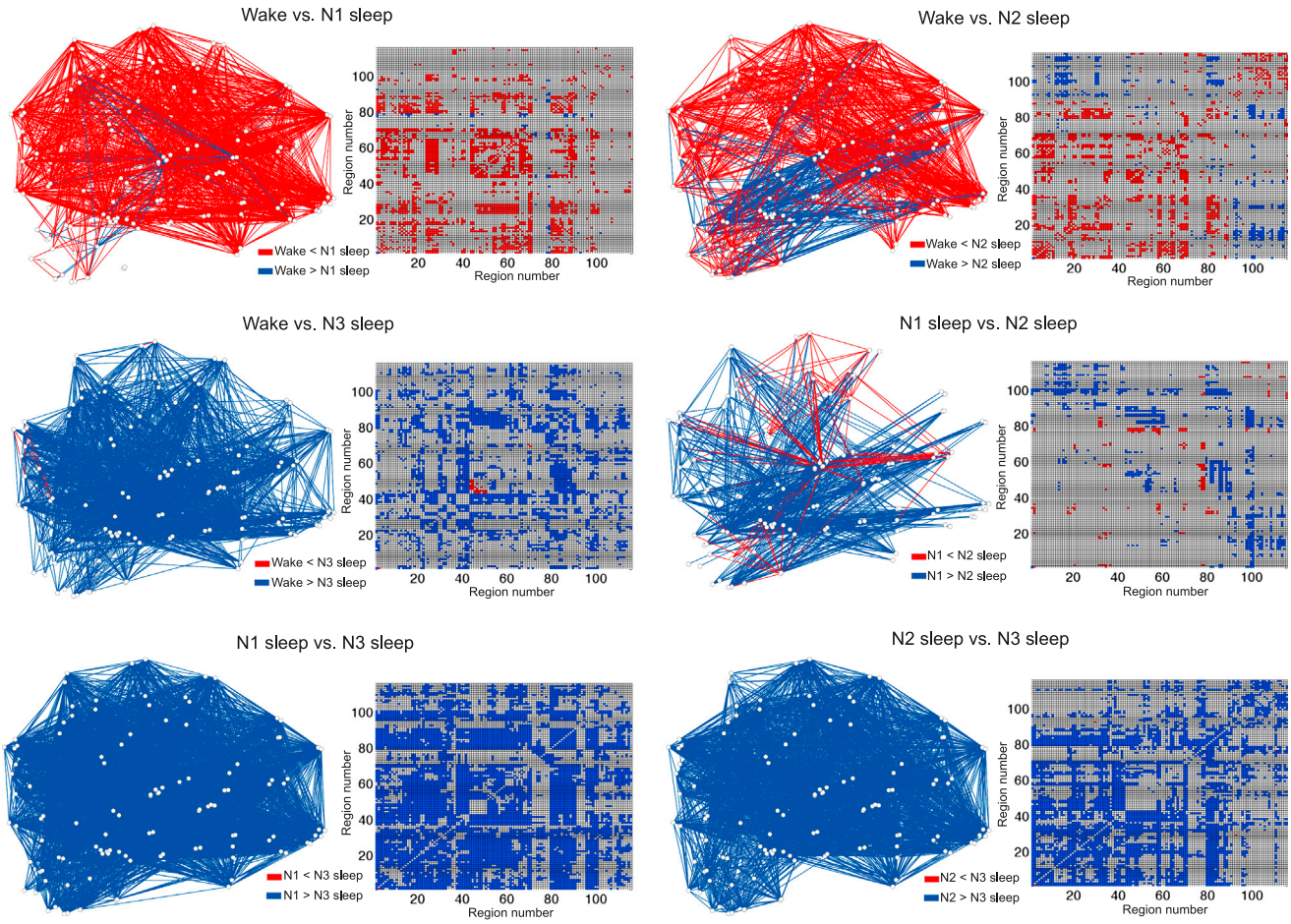

Figure 2. Large-Scale Functional Connectivity Patterns Identified for EEG-Defined Sleep Stages and Used to Classify NREM Sleep Stages from fMRI Data

For each one of the six possible pairs (permutation) of sleep stages, significantly different ($p < 0.05$, one-tailed Student's t test, Bonferroni corrected) functional connections are shown as a graph (or network; with node coordinates located at the center of mass of each AAL region) and in matrix form (with rows and columns corresponding to different AAL regions and each intersection representing a functional connection). Region codes and coordinates can be found in Table S1.

In Figure 4C, the probability of finding an awake subject as a function of time is shown, both for the Frankfurt data set and separately for every fMRI center forming the Connectome data set. Because this data set did not include EEG data, it was impossible to apply the gold standard polysomnography based on the AASM rules to detect the presence of sleep. However, if the SVM classifier correctly infers the sleep stage from fMRI functional connectivity data, then it can be expected that the probability of finding an asleep subject increases over time (and vice-versa for the probability of finding an awake subject). This heuristic was quantified in two ways. First, for each subject, the total amount of sleep (normalized by total scanning time) in the first and second half of the scanning session was computed (note that according to Figure 1B this heuristic is only valid for the beginning of the experiment, i.e., during the first ≈20 min), revealing that subjects were more likely to be asleep during the second part of the experiment than the first ($p = 0.0048$, Student's t test) (Figure 4D). Second, for each center, a linear function was fitted to the wakefulness probability as a function of time. A significant negative slope implies that, as the experiment progresses, it becomes more unlikely to find an awake subject. Results for all fMRI centers are presented in Figure 4E, revealing that the majority (30 out of 38) of centers presented a negative slope. Across the whole sample, the mean slope values were significantly smaller than zero ($p < 10^{-5}$, Student's t test).

It can also be expected that instructing subjects to keep their eyes open during the experiment results in a decreased amount of sleep. From the available data in the 1000 Functional Connectomes Project website, fMRI centers were divided into three groups: eyes open ("eye" symbol in Figure 4C), eyes open and fixation ("eye and cross" symbol in Figure 4C), and eyes closed (no symbol in Figure 4C). The mean amount of sleep in the group with eyes closed was higher than in the eyes open group (also including the fixation group), but nonsignificant ($p = 0.087$, Student's t test). However, all the fMRI centers scanning with eyes open and fixation had a very small amount of sleep. Not only subjects with eyes closed showed more sleep than the fixation group ($p = 0.036$, Student's t test) but the group with eyes

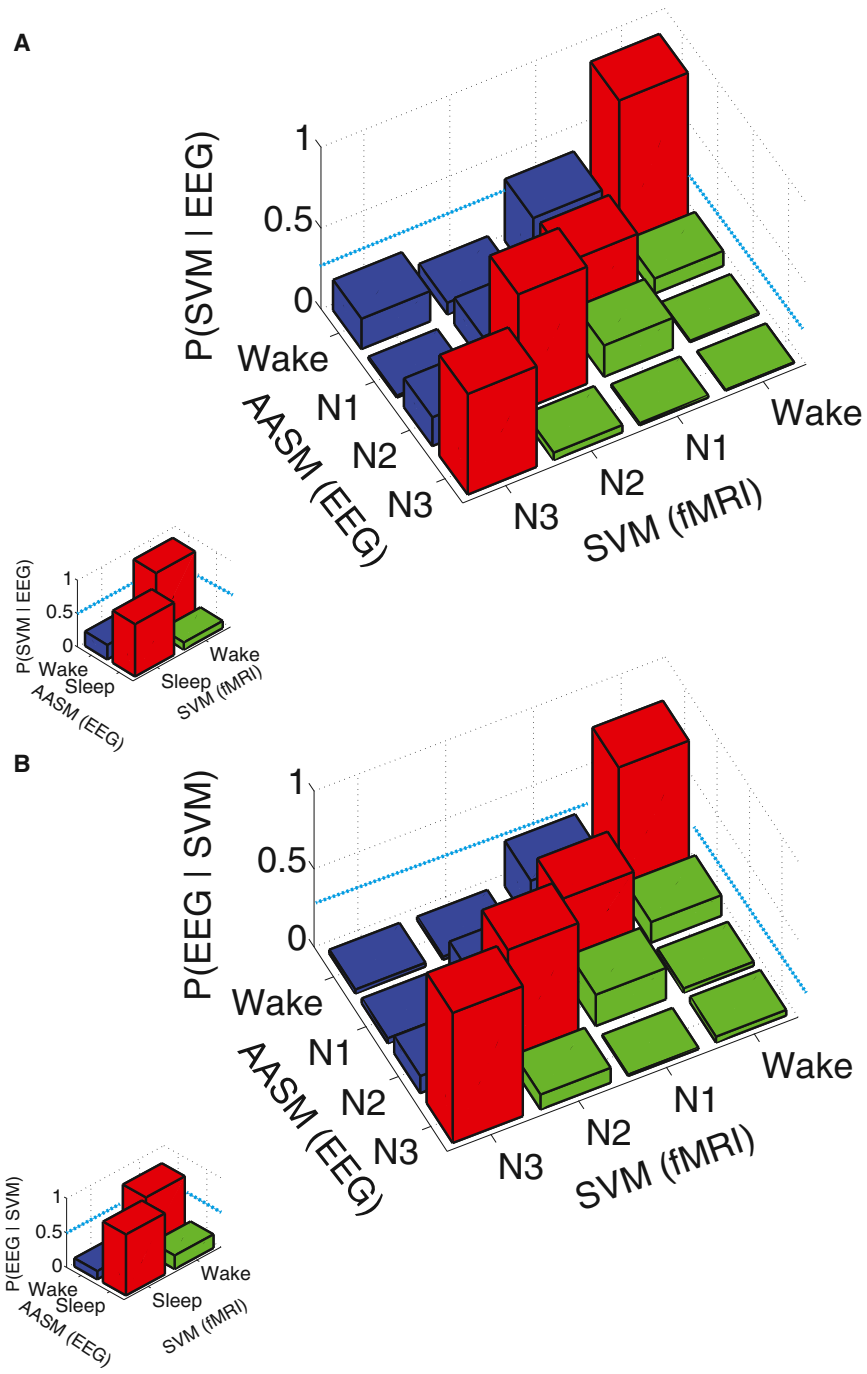

Figure 3. SVM Classifier Accurately Decodes Sleep from fMRI Data

(A) Probability of detecting the different NREM sleep stages with the SVM classifier given the EEG-based AASM scoring result, $P(SVM_i|EEG_j)$.

(B) Probability of NREM sleep stages, as detected by EEG-based AASM scoring rules, given different SVM outputs, $P(EEG_i|SVM_j)$. Insets: results of the binary wakefulness versus sleep classification are shown (i.e., with all sleep stages pooled together). Bars representing correct classifications are colored in red (diagonal), representing misclassifications toward less sleep depth in green and toward higher sleep depth in blue. In all panels, light blue dashed lines indicate the chance accuracy level.

open and without fixation also did ($p = 0.012$, Student's t test), suggesting that fixation supports the maintenance of wakefulness in a resting-state setting.

Mining Sleep from the Connectome Data Set

In order to assess not only the plausibility of correct SVM classification, we further assessed its validity: we looked at properties of the "estimated" sleep stage-specific hemodynamic signals, i.e., variance and functional connectivity of the hypothalamus. The latter region was not included in the SVM classification procedure and hence precluded circularity of the approach. We checked whether we could reproduce typical features specific for the different sleep stages as described in the neuroimaging literature previously (Horovitz et al., 2008; Tagliazucchi et al., 2013b; Kaufmann et al., 2006; Laufs et al., 2007)

For the respective analysis to be statistically unbiased and straightforward, we required paired data, and we thus screened the Connectome data set for contiguous epochs of sleep lasting longer than 2 min and selected only those from subjects having one epoch of wakefulness and one epoch of NREM sleep. This resulted in 97 wakefulness-N1 pairs, 24 wakefulness-N2 pairs, and 3 wakefulness-N3 pairs. Using this data, hypothalamic (MNI coordinates [−2,−10,−10]) functional connectivity maps and maps of BOLD signal variance were computed. Analogous computations were performed for the Frankfurt data set (sleep epochs selected via AASM sleep staging rules).

For both data sets, a comparison between wakefulness and sleep was performed, with the resulting statistical parametric maps shown in Figure 5. The maps obtained from the Frankfurt data set were thresholded at $p < 0.001$, those obtained from the Connectome data set at $p < 0.01$. We did not correct for multiple comparisons, given our regionally specific hypotheses; however, we report all voxels to illustrate the high spatial specificity of the response profiles. Very similar maps were obtained, revealing a decoupling of the hypothalamus from frontal, parietal and temporal cortices during N2 sleep (Figure 5A) and increased BOLD signal variance in motor and sensory cortices during N1 and N2 sleep compared to wakefulness (Figure 5B). While the

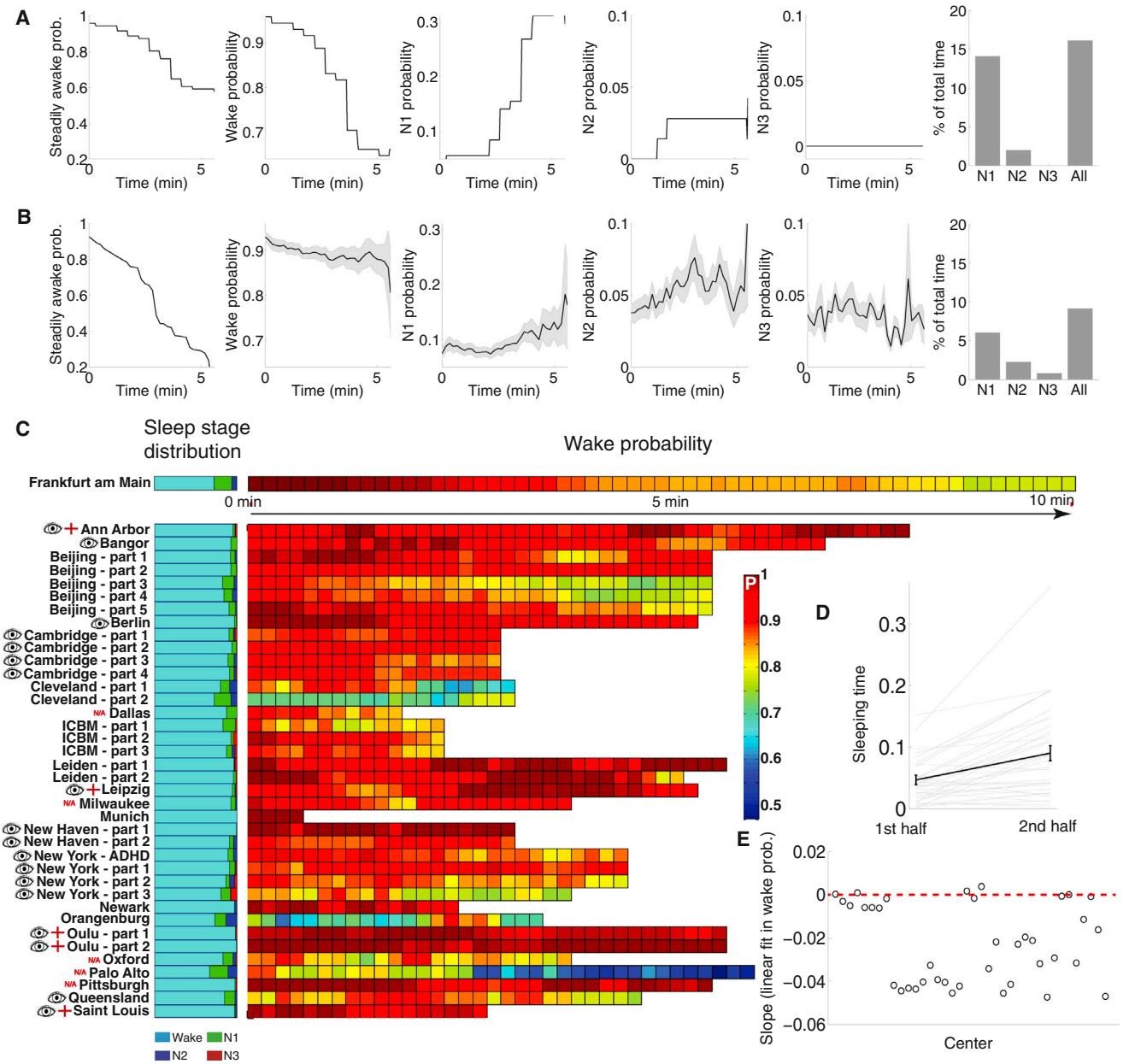

Figure 4. Subjects in the Connectome Data Set Are More Likely to be Asleep as the Resting-State Experiment Progresses

(A) Probabilities of steady wakefulness, of finding an awake subject and a subject in one of each of all three NREM sleep stages, the total time spent in N1, N2, and N3 sleep and in all sleep stages combined. Results are for the Frankfurt data set.

(B) Same plots as in (A), but for the Connectome data set (mean ± SEM, computed across all fMRI centers).

(C) Total time spent in the different NREM sleep stages (left) and wakefulness probability as a function of time (right). Results are presented for the Frankfurt data set and for all individual fMRI centers contributing to the Connectome data set. An eye next to the fMRI center name indicates an experiment with eyes open, an eye plus a cross indicates eyes open and fixation, and "N/A" indicates lack of data.

(D) Average sleeping time (normalized by scanning length) of subjects in the Connectome data set during the first and second half of the scan (individual data in gray and mean ± SEM in black).

(E) Slope obtained from fitting a linear function in the wakefulness probability versus time function of each fMRI center. A negative slope indicates that the likelihood of finding an awake subject decreases with time.

patterns were very similar for the two data sets, lower statistical power was obtained in the data extracted from the Connectome data set, possibly reflecting the inclusion of misclassified epochs.

Reconfiguration of Major Intrinsic Connectivity Networks during Sleep

To deepen the neurobiological implication of our findings, we studied how sleep impacts on intrinsic connectivity network

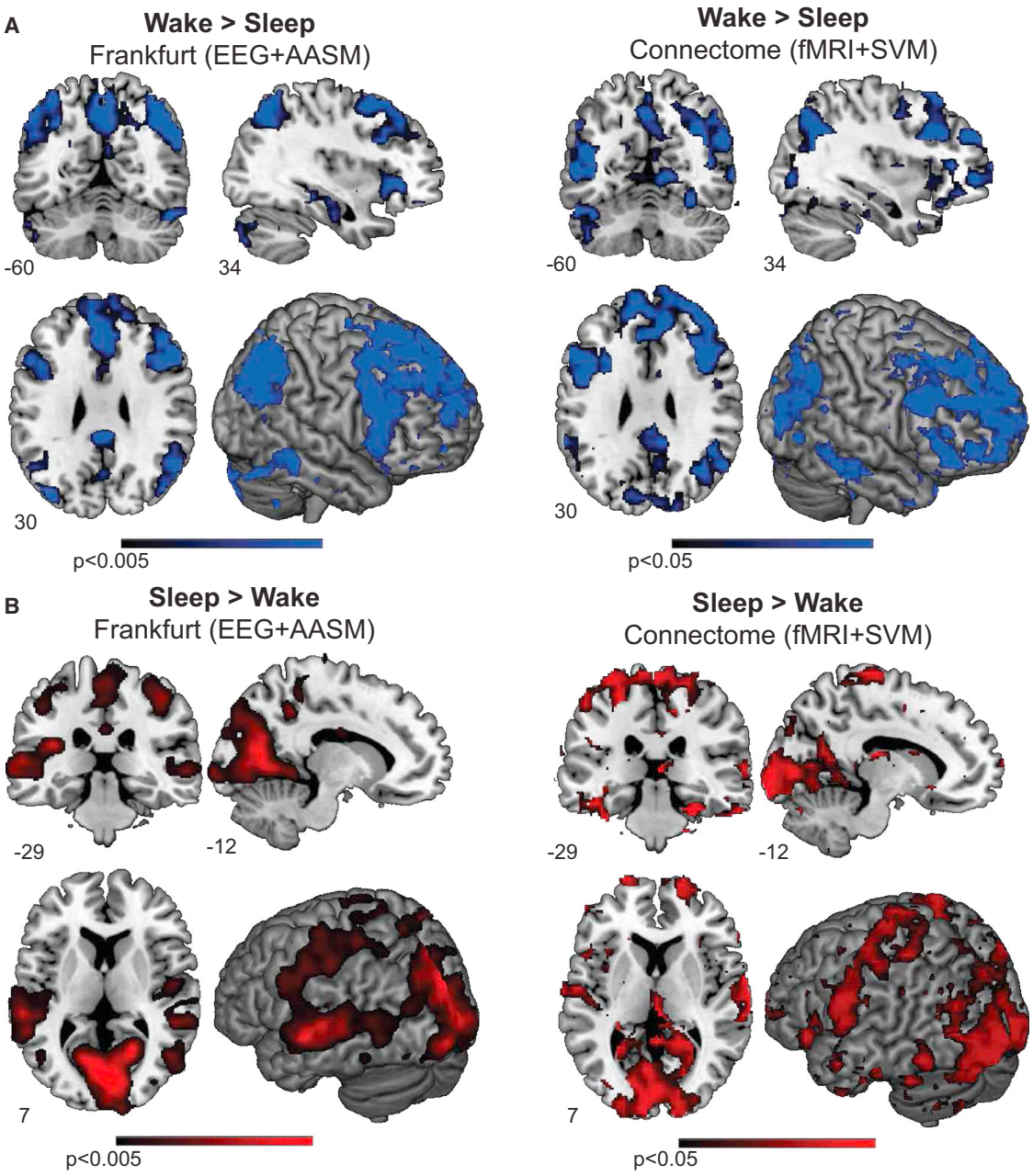

Figure 5. Changes in BOLD Functional Connectivity and Variance Are Typical, Sleep Stage Specific and Match between the EEG- and the SVM-Sleep-Scored Data sets

(A) Left: decreased functional connectivity between hypothalamus and frontal, parietal, and temporal cortices during N2 sleep (gold standard polysomnographic sleep scoring, Frankfurt data set). Right: similar pattern of decreased hypothalamic connectivity observed in N2 sleep (SVM classifier, Connectome data set). (B) Left: increased BOLD signal variance in sensory and motor cortices during N1 and N2 sleep, results for the Frankfurt data set (AASM scoring). Right: similar pattern of increased BOLD signal variance, data extracted from the Connectome data set using the SVM classifier. The maps obtained from the Frankfurt data set were thresholded at $p < 0.001$, those obtained from the connectome data set at $p < 0.01$.

(ICN) functional connectivity during different sleep stages (see also the Supplemental Experimental Procedures). In Figure 6, we show results for functional connectivity changes in auditory, default mode (DMN) and executive (CEN) ICN, and for N1 and N2 sleep versus wakefulness. An expanded presentation of the results is shown in Figures S2–S4. Between the regions constituting classical ICN, in N1 we found mainly increases in functional connectivity compared to wakefulness (with exceptions within the DMN and CEN), whereas in N3 it was almost exclusively decreases. N2 exhibited intermediate characteristics. In N1 sleep, temporal regions including both Heschl's and superior temporal gyri functionally connected more strongly to other

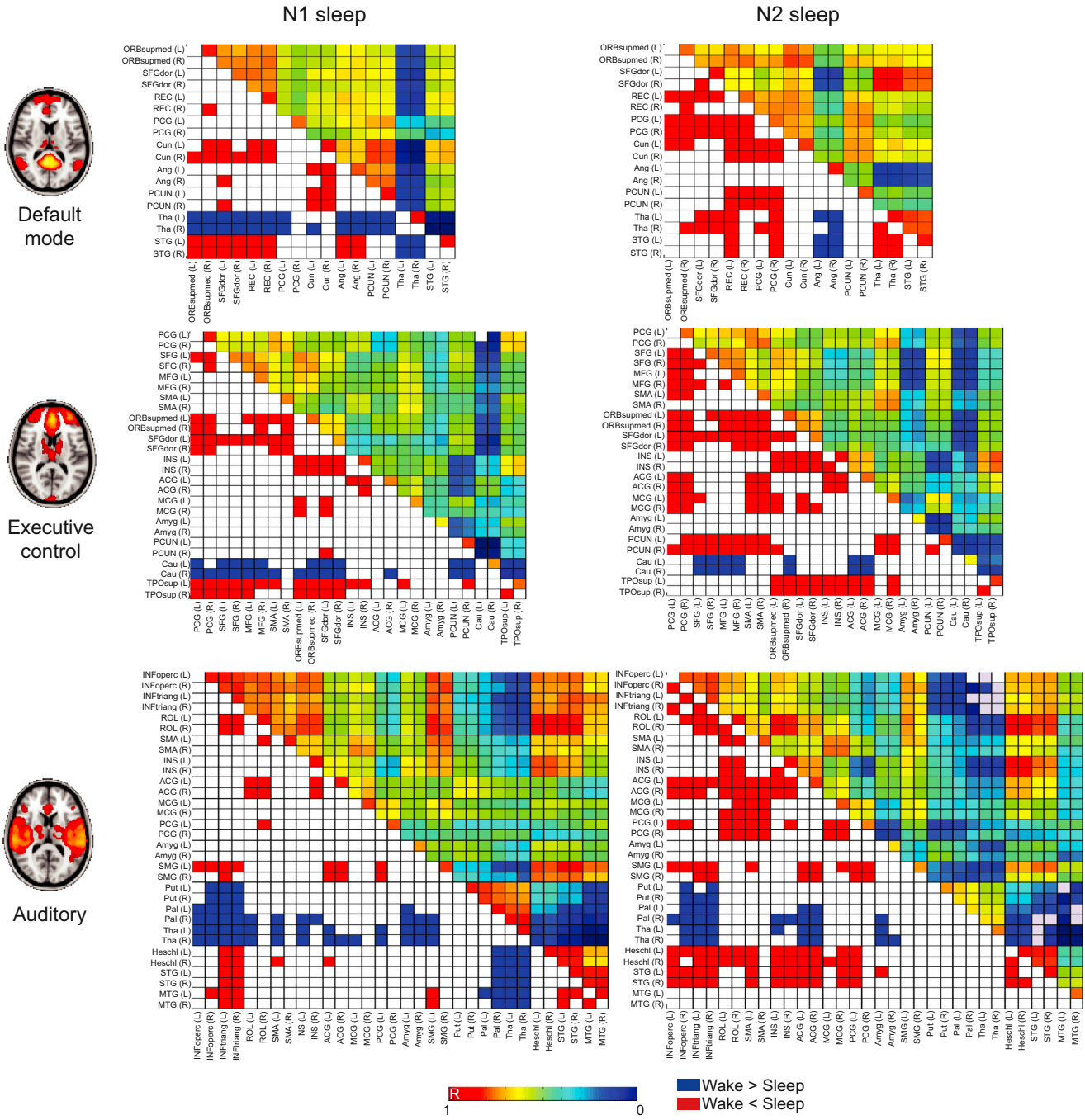

Figure 6. Default Mode, Executive, and Auditory ICN Are Reconfigured during N1 and N2 Sleep

Mean correlation values (upper diagonal) of all cortical and subcortical regions comprising default mode, executive and auditory ICN during N1 and N2 sleep. Below the diagonal, significant differences in correlation values between N1, N2 sleep, and wakefulness are shown ($p < 0.05$, Bonferroni corrected). See the Supplemental Information for more comprehensive results.

temporal and superior frontal regions. Within the DMN, thalamus and superior temporal gyrus almost traded places with respect to their functional connectivity to orbito and superior frontal regions and the gyrus rectus: reciprocally, their connectivity became stronger while the thalamic links became weaker.

DISCUSSION

The number of fMRI resting-state studies grows exponentially (Birn, 2012) with over 600 studies published on the topic in 2012 (PubMed, search terms "fMRI resting state"). Fluctuations

in resting-state activity are well known, but their biological origins are not equally well understood. We demonstrate fluctuations in wakefulness as one potential contributing neuronal source. Of our 71 subjects studied at rest simultaneously with EEG and fMRI, within 5 min <50% remained stably awake (Figure 1). Instead, subjects succumbed to sleep pressure resulting in their functional brain architecture to change substantially (Figures 2 and 6). We could generalize this observation to a global cohort of 1,147 subjects confirming quickly fluctuating wakefulness (30% not stably awake for longer than 3 min) as a universal principle in human resting-state studies (Figure 4). Based on fMRI-derived sleep staging, in these 1,147 data sets, we reproduced connectivity and variance patterns specific to EEG-defined sleep stages (Tagliazucchi et al., 2013b) (Figure 5). This independent reproduction of functional brain network behavior is confirmatory evidence for the reliability of our classifier-based sleep staging in the 1,147 subjects.

Sensitivity and Specificity of Resting-State fMRI as a Possible Biomarker

Resting-state research is considered by some as a promising avenue to identify biomarkers in disease. Efforts—including political and financial—have been made to push forward this line of research (Castellanos et al., 2013; Greicius, 2008; Kaiser, 2013; Kandel et al., 2013; Sporns, 2012; Van Essen and Ugurbil, 2012). Our findings impact hugely on the success of these efforts in the following aspects: (1) false negatives: given that "the resting state" in fact is a variable mixture of several distinctly different brain states, attempts to characterize the resting state are prone to be compromised by the variability induced by the state of wakefulness that is ignored when analyzing the collapsed states as a single one, and (2) false positives: if two conditions are compared, e.g., a patient cohort versus a control group, which systematically differ in the propensity of sleep, differences in network characteristics imposed by different degrees of wakefulness might be misinterpreted as induced by the disease. It is well conceivable that sleep pressure and hence its propensity in pathological conditions differs systematically between healthy and disease-struck subjects (both in the form of increased sleepiness or insomnia). This could arise either as inherent to the condition itself or due to related active medical treatment (Ford and Kamerow, 1989; Mayer et al., 2011; Sateia et al., 2000). Equally, patients might exhibit more extreme behavior—ranging from anxiety because of the examination and its resulting implications, or relief after a sleepless night before the test—than control subjects who might generally exhibit a more balanced state.

In line with these considerations are the known high individual variability (Mueller et al., 2013) and e.g., observations from the ADHD-200 Global Competition attempting to promote discovery science by sharing of resting-state fMRI data (Castellanos et al., 2013). Given the goal of classifying ADHD versus healthy controls, the best classifier was not based on the resting-state fMRI data. Instead, the best classification was achieved by taking advantage of the male predominance and the tendency to manifest lower IQ characterizing ADHD (Brown et al., 2012; The HD-200 Consortium, 2012). The relative failure of using resting-state fMRI measures might be explained—among others (Murphy et al., 2013)—by heterogeneous brain states associated with fluctuating wakefulness, as pointed out in the preceding paragraph.

An example for a systematic wakefulness confound in a resting-state study was given by Diaz et al. (2013) who suggested that sleepiness may partially explain a resting-state EEG profile previously associated with Alzheimer's disease. Interestingly, the same study showed that the structure of cognition was similar during resting-state fMRI and EEG and that the test-retest correlations were high for all dimensions of a 50 item self-report survey (the Amsterdam Resting State Questionnaire) including Discontinuity of Mind, Theory of Mind, Self, Planning, Sleepiness, Comfort, and Somatic Awareness (Diaz et al., 2013). This argues for the possibility that fluctuations in wakefulness might contribute more to variability in the resting state than the individual's "mental state."

N1: Mere Cognitive Shift or Proper Sleep Stage?

We found that during a typical fMRI resting-state experiment the intrusion of N1 sleep is common. Some may wonder whether N1 sleep might reasonably be considered a natural part of the variation in naturalistic cognition. Our results indicate that N1 sleep is a neurophysiologically distinct brain state, which cannot be put in equal footing with other states naturally occurring during wakeful rest. We provide an extended discussion in the Supplemental Information.

Effect of Fixation Condition on Brain State

Other examples suggestive of a wakefulness bias in resting-state experiments are the systematic differences between eyes-open and eyes-closed resting-state studies, as reviewed in Castellanos et al. (2013). Systematic increases in BOLD signal variance in occipital regions during eyes-closed compared to fixation have been highlighted by Bianciardi et al. (2009a) and are equally observed in sleep compared to wakefulness (Horovitz et al., 2008; Tagliazucchi et al., 2013b) as well as in our present study (Figure 5).

While according to our results, subjects with their eyes open did not fall asleep significantly less than those with their eyes closed, an additional fixation challenge significantly increased the likelihood of subjects staying stably awake. However, such a task with its respective effect on the brain state undermines a fundamental motivation of resting-state experiments: to study subjects who cannot engage in a paradigm (e.g., patients) and are not supposed to exhibit any (unknown) strategic behavior (Castellanos et al., 2013). Having demonstrated that sleep pressure is immense in fMRI resting-state studies, we can infer that in order to adhere to such a fixation task, individuals must pursue some strategy to fight sleep and that those who do not, are the ones to most likely fall asleep.

A Neuronal Bias in Addition to Physiological Confounds

A number of confounds of resting-state fMRI studies have been described previously, such as subject motion, thermal, cardiac, pulsation, and respiratory noise introducing variance into the data of at least the size as that thought to originate from neuronal activity fluctuations. These have been reported as <3% of the BOLD baseline amplitude (Bianciardi et al., 2009b) and modeling

strategies have been proposed to reduce confounding effects (Murphy et al., 2013). However, these latter sources of fMRI signal variance differ from the confound sleep in the following key aspects: different sleep stages (1) substantiate in neuronal activity and—directly associated—in BOLD signal changes, and (2) modify connectivity patterns of the whole brain with variable regional emphasis. The respective comprehensive details can be found in Figures 2, 5, and 6, and their exhaustive discussion deserves a new work by itself.

Sleep-Induced Connectivity Changes in Intrinsic Connectivity Networks

Nevertheless, in order to strike a balance between the neuroanatomical discussion of our biologically inherently interesting findings and secondary space limitations of this Article, we focus here on changes in connectivity with particular reference to canonical ICN (or resting-state networks [RSNs]) (Figure S1). This includes regions involved in motor function, visual processing, executive functioning (CEN), auditory processing, and the so-called default-mode network (DMN) (Damoiseaux et al., 2006).

In line with previous findings, we interpret the net reduction in connectivity observed during deep sleep as ceasing brain interregional cross talk, i.e., a loss of global integration well in line with a phenotypically concomitant reduction in consciousness (Massimini et al., 2005; Tagliazucchi et al., 2013a, 2013b). The distributed thalamic "disconnection" is a general feature observable when comparing thalamic links during wakefulness and N1 and parallels electrophysiological observations of early thalamic deactivation at sleep onset (Magnin et al., 2010). In the same study, Magnin et al. (2010) present evidence that complexity of cortical activity at sleep onset persists beyond that of already decreasing thalamic activity. Our data might represent the functional imaging correlate of this behavior when comparing N1 and N2 to wakefulness: within the ICNs of interest, during N1 the majority of corticocortical connectivity does not change. The same observation holds during N2 with the following exception: regions of the anterior- and midcingulate cortex (Figures 6, S2, and S4, see the sensorimotor ICN, auditory ICN, and CEN) exhibit connectivity changes. These are associated with and likely linked to activity increases in these regions related to sleep paroxysmal events, i.e., spindles, K-complexes, and vertex sharp waves (Jahnke et al., 2012; Stern et al., 2011). It is only in N3 that the functional connectivity shows decreases with virtually no concomitant increases in functional connectivity (Figure S4). In N3, the regions that exhibited connectivity increases during N2 compared to wakefulness, e.g., the cingulate cortex, do not show significant connectivity decreases in N3 compared to wakefulness. This might be explained by functional synchronization during sleep paroxysmal events only now from a generally lower connectivity baseline. This would result in a failure of these regions to be detected as significant absolute connectivity increases despite an increase in functional connectivity relative to baseline N3 connectivity.

Horovitz et al. (2009) and Vanhaudenhuyse et al. (2010) described decreases in functional connectivity within the DMN during sleep (Horovitz et al., 2009) and in other conditions associated with reduced consciousness (Vanhaudenhuyse et al., 2010) and established a link between the latter and functional decoupling within the DMN. We can reproduce their findings of decreased functional connectivity in deeper sleep compared to wakefulness. Having extended the functional connectivity analysis to the whole brain and across all NREM sleep stages, we observed that fewer connections change in the DMN from W to N3 than in the other canonical ICN. This comparably moderate decoupling is indicative of a special role the DMN might play in the context of consciousness compared to other ICN. At the same time, it suggests that mechanisms other than within-ICN reductions in functional connectivity might be relevant. Using graph analysis based on whole brain functional connectivity, we found that modularity, a spatial measure of functional segregation, generally increased across the brain with deepening sleep (Tagliazucchi et al., 2013a). Of note, examining also the temporal integration of information, it was decreased to a much larger degree in the DMN (and the attentional network) than in primary sensory networks (Tagliazucchi et al., 2013b). These findings are consistent with the information integration theory of consciousness brought forward by Tononi (2004) both in the spatial and temporal domains, although examination of causal influences is required to fully support the aforementioned theory.

In the context of this study, we hence summarize that the qualitative operating mode of the brain with its functional connectivity architecture changes with deepening sleep and concomitant consciousness reduction (Boly, 2011; Boly et al., 2012; Horovitz et al., 2009; Massimini et al., 2005; Olbrich et al., 2009; Picchioni et al., 2013; Sämann et al., 2011; Tagliazucchi et al., 2012a, 2012b, 2013a, 2013b; Vincent et al., 2007).

We have also obtained ICN connectivity for the different NREM sleep stages with and without removal of physiological noise time series via regression (Glover et al., 2000). While we observed similar patterns with and without physiological noise regression (see Figures S2 and S3 for results without regression, Figure S4 for results with regression, and Figure S5 for the comparison between both), the main effect of cardiac and respiratory noise can be summarized as a general increase of functional connectivity across the brain with only few significant differential regional effects. The described effects become less pronounced with deepening sleep. The near absence of physiological noise-induced effects in deep sleep together with the sparse differential effects during wakefulness and light sleep lend further support to the hypothesis of a true neural origin of spontaneous BOLD functional connectivity fluctuations.

Brain State versus Disease Marker

Cognitive neuroscience makes use of the assumption that brain function can be studied by challenging individuals with paradigms designed to evoke certain behavior. This approach must fail in brain states in which subjects cannot exhibit actively and consciously differentiated performance in response to any such task. While during wakefulness such behavior interacts with or modifies resting-state brain activity (Raichle and Snyder, 2007; Zhang and Raichle, 2010), in deeper sleep with reduced consciousness, the homeostatic brain activity is the resting-state activity characteristically observed in each sleep stage, with only very limited interaction or modification inducible by

any external (arousing) stimulus (Czisch et al., 2002; Portas et al., 2000). Such interaction between ongoing and externally induced activity is paroxysmal in nature an can be observed during sleep stages N1 and N2 in the form of K-complexes and vertex sharp waves and their fMRI correlates (Jahnke et al., 2012; Stern et al., 2011). It is not continuously interwoven as is thought to be the case for the wakeful brain (Raichle and Snyder, 2007). In deeper sleep, externally induced modification of brain function is restricted further (Czisch et al., 2002; Portas et al., 2000) and corresponds well to the loss of integration of brain activity both spatially and temporally (Tagliazucchi et al., 2013a, 2013b), which is in line with theories of consciousness proposing this to be a prerequisite for conscious processing (Tononi, 2004).

We do not challenge the assumption that characteristics in resting-state brain activity of patient groups exist and could serve as biomarkers. However, their identification requires sleep stage-specific analysis approaches, and we currently do not know how prominent such particularities are compared to the fundamental changes associated with changes in wakefulness. While we are confident that our classifier (Tagliazucchi et al., 2012a) based on functional connectivity reliably identified sleep in the cohort of healthy volunteers (Figure 3), it is conceivable that in a patient cohort truly disease-specific network alterations might be misclassified as being sleep-associated, especially in conditions characterized by impaired consciousness. Hence, in fMRI resting-state studies, an independent measure of sleep should be obtained, e.g., simultaneously recorded polysomnographic EEG.

EEG Features Sensitive to Wakefulness Levels Were Linked to Hemodynamic Resting-State Patterns

Hemodynamic fluctuations in resting-state networks were associated with EEG features such as typical resting-state topographies (Brodbeck et al., 2012; Musso et al., 2010; Van de Ville et al., 2010) or oscillations in EEG frequency bands (Laufs et al., 2003a, 2003b, 2006; Olbrich et al., 2009) also used clinically for sleep staging (AASM, 2007). These studies demonstrate a link between different observed neuronal activity patterns and vigilance levels and hence support the notion that resting-state fluctuations could reflect at least in part the switching of brain activity between different sleep stages. Of such, more can be characterized than those classically used and pragmatically defined by AASM criteria (AASM, 2007; Davis et al., 1937; Fox et al., 2006; Loomis et al., 1935; Roth, 1961) suggesting the possibility of frequent sleep state changes as a correlate of resting-state fMRI and EEG fluctuations.

Conclusions

In conclusion, in order to increase both sensitivity and specificity of resting-state fMRI studies, we provide evidence that in analyses based on functional connectivity, the brain state should be determined and accounted for in the related analysis strategies and results should be critically reviewed for false positives originating from unstable vigilance levels, especially if the state of wakefulness remains obscure. Otherwise, the validity of results derived from potentially powerful collaborative databases is at risk. The methods and principles introduced in this paper could be extended to more precisely restrict the type of wakeful rest under study. Also, future studies should address whether the slow fluctuations in fMRI resting-state activity are identical to fluctuations in vigilance levels or to which degree they originate independently.

EXPERIMENTAL PROCEDURES

EEG-fMRI Acquisition and Artifact Correction

EEG via a cap (modified BrainCapMR, Easycap) was recorded during fMRI acquisition (1,505 volumes of T2*-weighted echo planar images, TR/TE = 2,080 ms/30 ms, matrix 64 × 64, voxel size 3 × 3 × 2 mm^3, distance factor 50%; field of view [FOV] 192 mm^2) at 3 T (Siemens Trio) with an optimized polysomnographic setting (chin and tibial electromyography [EMG], electrocardiography [ECG], electrooculography [EOG] recorded bipolarly [sampling rate 5 kHz, low pass filter 1 kHz], 30 EEG channels recorded with FCz as the reference [sampling rate 5 kHz, low pass filter 250 Hz], and pulse oximetry, respiration recorded via sensors from the Trio [sampling rate 50 Hz]) and MR scanner compatible devices (BrainAmp MR+, BrainAmp ExG; Brain Products).

MRI and pulse artifact correction were performed based on the average artifact subtraction (AAS) method (Allen et al., 1998) as implemented in Vision Analyzer2 (Brain Products) followed by objective (CBC parameters, Vision Analyzer) ICA-based rejection of residual artifact-laden components after AAS resulting in EEG with a sampling rate of 250 Hz. Good quality EEG was obtained, which allowed sleep staging by an expert according to the AASM criteria (AASM, 2007).

Subjects and Data Set

A total of 71 subjects were selected from a larger data set on the basis of successful EEG, EMG, fMRI, and physiological data recording and quality (written informed consent, approval by the local ethics committee). All subjects were scanned during the evening and instructed to close their eyes and lie still and relaxed. The Connectome data set was downloaded from the 1000 Functional Connectomes Project online database (http://fcon_1000.projects.nitrc.org). Demographics, scanning parameters, and experimental conditions are described in the Supplemental Information (Table S2).

Data Preprocessing

Using Statistical Parametric Mapping (SPM8) EPI data were realigned, normalized (MNI space) and spatially smoothed (Gaussian kernel, 8 mm^3 full width at half maximum). Data were band-pass filtered in the range 0.01–0.1 Hz using a sixth order Butterworth filter. The same procedure was applied to the Frankfurt data set and the Connectome data set.

Training/Testing Sets and Feature Selection

A group of 55 subjects was formed out of the original data set of 71 subjects (by excluding subjects who did not fall asleep) and then further (randomly) subdivided into two sets: a training set of 30 subjects and a testing set of 25 subjects. In the training set, fMRI data corresponding to different sleep stages was partitioned into nonoverlapping 2 min windows, yielding 265 2 min epochs of wakefulness, 120 epochs of N1 sleep, 105 epochs of N2 sleep, and 60 epochs of N3 sleep. Inside each window, the linear correlation between the mean BOLD signal of all 116 AAL regions (for region coordinates and names see Table S1 and Supplemental Information) was computed and for each possible pair of sleep stages an univariate feature selection was applied, discarding those connections which were not significantly different in their correlation value ($p < 0.05$, Bonferroni corrected), resulting in the networks shown in Figure 2. Only these connections were used to train the SVM classifier. The testing set was used to evaluate the classifier performance using a 2 min sliding window to compute correlations.

SVM Classifier

An introduction to SVM and a detailed explanation of the methods can be found in Tagliazucchi et al. (2012a). The procedure employed here is similar to that in Tagliazucchi et al. (2012a), with the main difference being the use of the AAL template in combination with a univariate feature selection to identify relevant connections in the training data. For each binary problem

(i.e., discriminating between each pair of sleep stages) a SVM was trained using the SVM-KM toolbox (http://asi.insa-rouen.fr/enseignants/~arakoto/toolbox/index.html) with a radial basis function (RBF) kernel, given by $K(x,y) = \exp(-\gamma|x - y|^2)$. The two parameters (the kernel parameter γ and C, a constant representing a misclassification penalty) were optimized using a 5-fold cross validation procedure. Parameters were varied over an exponential grid with values expressed as 2^x, with $x = -25,\ldots, 25$. Binary SVMs were combined into a multiclass SVM using a one-against-one scheme.

SUPPLEMENTAL INFORMATION

Supplemental Information includes Supplemental Experimental Procedures, six figures, and two tables and can be found with this article online at http://dx.doi.org/10.1016/j.neuron.2014.03.020.

ACKNOWLEDGMENTS

This work was funded by the Bundesministerium für Bildung und Forschung (grant 01 EV 0703) and the LOEWE Neuronale Koordination Forschungsschwerpunkt Frankfurt (NeFF). We thank Helmuth Steinmetz, Astrid Morzelewski, Kolja Jahnke, Sandra Anti, Ralf Deichmann, and Steffen Volz for extensive support and our volunteers for participation in the study. We are grateful to the International Neuroimaging Data-Sharing Initiative (INDI), especially Michael Milham, for making the 1000 Functional Connectomes Project data set publicly available. We thank Thomas Sattler for excellent IT infrastructure maintenance, without which the analysis of this data would not have been possible. Finally, we thank the anonymous reviewers for their constructive suggestions, which at times found literal entrance to this manuscript version.

Accepted: March 13, 2014
Published: May 7, 2014

REFERENCES

AASM (2007). The AASM Manual for the Scoring of Sleep and Associated Events: Rules, Terminology and Technical Specifications. (Westchester: American Academy of Sleep Medicine).

Alivisatos, A.P., Chun, M., Church, G.M., Greenspan, R.J., Roukes, M.L., and Yuste, R. (2012). The brain activity map project and the challenge of functional connectomics. Neuron *74*, 970–974.

Allen, P.J., Polizzi, G., Krakow, K., Fish, D.R., and Lemieux, L. (1998). Identification of EEG events in the MR scanner: the problem of pulse artifact and a method for its subtraction. Neuroimage *8*, 229–239.

Baliki, M.N., Geha, P.Y., Apkarian, A.V., and Chialvo, D.R. (2008). Beyond feeling: chronic pain hurts the brain, disrupting the default-mode network dynamics. J. Neurosci. *28*, 1398–1403.

Baumann, H., Baumann, R., Gurk, C., and Wolter, F. (1968). Electrophysiological studies of central nervous performance during monotony. Electroencephalogr. Clin. Neurophysiol. *24*, 259–273.

Bianciardi, M., Fukunaga, M., van Gelderen, P., Horovitz, S.G., de Zwart, J.A., and Duyn, J.H. (2009a). Modulation of spontaneous fMRI activity in human visual cortex by behavioral state. Neuroimage *45*, 160–168.

Bianciardi, M., Fukunaga, M., van Gelderen, P., Horovitz, S.G., de Zwart, J.A., Shmueli, K., and Duyn, J.H. (2009b). Sources of functional magnetic resonance imaging signal fluctuations in the human brain at rest: a 7 T study. Magn. Reson. Imaging *27*, 1019–1029.

Birn, R.M. (2012). The role of physiological noise in resting-state functional connectivity. Neuroimage *62*, 864–870.

Birn, R.M., Diamond, J.B., Smith, M.A., and Bandettini, P.A. (2006). Separating respiratory-variation-related fluctuations from neuronal-activity-related fluctuations in fMRI. Neuroimage *31*, 1536–1548.

Birn, R.M., Murphy, K., and Bandettini, P.A. (2008). The effect of respiration variations on independent component analysis results of resting state functional connectivity. Hum. Brain Mapp. *29*, 740–750.

Biswal, B.B., Mennes, M., Zuo, X.N., Gohel, S., Kelly, C., Smith, S.M., Beckmann, C.F., Adelstein, J.S., Buckner, R.L., Colcombe, S., et al. (2010). Toward discovery science of human brain function. Proc. Natl. Acad. Sci. USA *107*, 4734–4739.

Boly, M. (2011). Measuring the fading consciousness in the human brain. Curr. Opin. Neurol. *24*, 394–400.

Boly, M., Perlbarg, V., Marrelec, G., Schabus, M., Laureys, S., Doyon, J., Pélégrini-Issac, M., Maquet, P., and Benali, H. (2012). Hierarchical clustering of brain activity during human nonrapid eye movement sleep. Proc. Natl. Acad. Sci. USA *109*, 5856–5861.

Brodbeck, V., Kuhn, A., von Wegner, F., Morzelewski, A., Tagliazucchi, E., Borisov, S., Michel, C.M., and Laufs, H. (2012). EEG microstates of wakefulness and NREM sleep. Neuroimage *62*, 2129–2139.

Brown, M.R., Sidhu, G.S., Greiner, R., Asgarian, N., Bastani, M., Silverstone, P.H., Greenshaw, A.J., and Dursun, S.M. (2012). ADHD-200 Global Competition: diagnosing ADHD using personal characteristic data can outperform resting state fMRI measurements. Front. Syst. Neurosci. *6*, 69.

Castellanos, F.X., Di Martino, A., Craddock, R.C., Mehta, A.D., and Milham, M.P. (2013). Clinical applications of the functional connectome. Neuroimage *80*, 527–540.

Christoff, K., Gordon, A.M., Smallwood, J., Smith, R., and Schooler, J.W. (2009). Experience sampling during fMRI reveals default network and executive system contributions to mind wandering. Proc. Natl. Acad. Sci. USA *106*, 8719–8724.

Czisch, M., Wetter, T.C., Kaufmann, C., Pollmächer, T., Holsboer, F., and Auer, D.P. (2002). Altered processing of acoustic stimuli during sleep: reduced auditory activation and visual deactivation detected by a combined fMRI/EEG study. Neuroimage *16*, 251–258.

Damoiseaux, J.S., Rombouts, S.A.R.B., Barkhof, F., Scheltens, P., Stam, C.J., Smith, S.M., and Beckmann, C.F. (2006). Consistent resting-state networks across healthy subjects. Proc. Natl. Acad. Sci. USA *103*, 13848–13853.

Davis, H., Davis, P.A., Loomis, A.L., Harvey, E.N., and Hobart, G. (1937). Changes in human brain potentials during the onset of sleep. Science *86*, 448–450.

Devor, A., Bandettini, P.A., Boas, D.A., Bower, J.M., Buxton, R.B., Cohen, L.B., Dale, A.M., Einevoll, G.T., Fox, P.T., Franceschini, M.A., et al. (2013). The challenge of connecting the dots in the B.R.A.I.N. Neuron *80*, 270–274.

Di Martino, A., Kelly, C., Grzadzinski, R., Zuo, X.N., Mennes, M., Mairena, M.A., Lord, C., Castellanos, F.X., and Milham, M.P. (2011). Aberrant striatal functional connectivity in children with autism. Biol. Psychiatry *69*, 847–856.

Di Martino, A., Yan, C.G., Li, Q., Denio, E., Castellanos, F.X., Alaerts, K., Anderson, J.S., Assaf, M., Bookheimer, S.Y., Dapretto, M., et al. (2013). The autism brain imaging data exchange: towards a large-scale evaluation of the intrinsic brain architecture in autism. Mol. Psychiatry. Published online June 18, 2013. http://dx.doi.org/10.1038/mp.2013.78.

Diaz, B.A., Van Der Sluis, S., Moens, S., Benjamins, J.S., Migliorati, F., Stoffers, D., Den Braber, A., Poil, S.S., Hardstone, R., Van't Ent, D., et al. (2013). The Amsterdam Resting-State Questionnaire reveals multiple phenotypes of resting-state cognition. Front. Hum. Neurosci. *7*, 446.

Ford, D.E., and Kamerow, D.B. (1989). Epidemiologic study of sleep disturbances and psychiatric disorders. An opportunity for prevention? JAMA *262*, 1479–1484.

Fox, M.D., and Raichle, M.E. (2007). Spontaneous fluctuations in brain activity observed with functional magnetic resonance imaging. Nat. Rev. Neurosci. *8*, 700–711.

Fox, M.D., Corbetta, M., Snyder, A.Z., Vincent, J.L., and Raichle, M.E. (2006). Spontaneous neuronal activity distinguishes human dorsal and ventral attention systems. Proc. Natl. Acad. Sci. USA *103*, 10046–10051.

Glover, G.H., Li, T.Q., and Ress, D. (2000). Image-based method for retrospective correction of physiological motion effects in fMRI: RETROICOR. Magn. Reson. Med. *44*, 162–167.

Greicius, M. (2008). Resting-state functional connectivity in neuropsychiatric disorders. Curr. Opin. Neurol. *21*, 424–430.

Gusnard, D.A., Raichle, M.E., and Raichle, M.E. (2001). Searching for a baseline: functional imaging and the resting human brain. Nat. Rev. Neurosci. *2*, 685–694.

Horovitz, S.G., Fukunaga, M., de Zwart, J.A., van Gelderen, P., Fulton, S.C., Balkin, T.J., and Duyn, J.H. (2008). Low frequency BOLD fluctuations during resting wakefulness and light sleep: a simultaneous EEG-fMRI study. Hum. Brain Mapp. *29*, 671–682.

Horovitz, S.G., Braun, A.R., Carr, W.S., Picchioni, D., Balkin, T.J., Fukunaga, M., and Duyn, J.H. (2009). Decoupling of the brain's default mode network during deep sleep. Proc. Natl. Acad. Sci. USA *106*, 11376–11381.

Jahnke, K., von Wegner, F., Morzelewski, A., Borisov, S., Maischein, M., Steinmetz, H., and Laufs, H. (2012). To wake or not to wake? The two-sided nature of the human K-complex. Neuroimage *59*, 1631–1638.

Kaiser, M. (2013). The potential of the human connectome as a biomarker of brain disease. Front. Hum. Neurosci. *7*, 484.

Kandel, E.R., Markram, H., Matthews, P.M., Yuste, R., and Koch, C. (2013). Neuroscience thinks big (and collaboratively). Nat. Rev. Neurosci. *14*, 659–664.

Kaufmann, C., Wehrle, R., Wetter, T.C., Holsboer, F., Auer, D.P., Pollmächer, T., and Czisch, M. (2006). Brain activation and hypothalamic functional connectivity during human non-rapid eye movement sleep: an EEG/fMRI study. Brain *129*, 655–667.

Laufs, H., Krakow, K., Sterzer, P., Eger, E., Beyerle, A., Salek-Haddadi, A., and Kleinschmidt, A. (2003a). Electroencephalographic signatures of attentional and cognitive default modes in spontaneous brain activity fluctuations at rest. Proc. Natl. Acad. Sci. USA *100*, 11053–11058.

Laufs, H., Kleinschmidt, A., Beyerle, A., Eger, E., Salek-Haddadi, A., Preibisch, C., and Krakow, K. (2003b). EEG-correlated fMRI of human alpha activity. Neuroimage *19*, 1463–1476.

Laufs, H., Holt, J.L., Elfont, R., Krams, M., Paul, J.S., Krakow, K., and Kleinschmidt, A. (2006). Where the BOLD signal goes when alpha EEG leaves. Neuroimage *31*, 1408–1418.

Laufs, H., Walker, M.C., and Lund, T.E. (2007). 'Brain activation and hypothalamic functional connectivity during human non-rapid eye movement sleep: an EEG/fMRI study'—its limitations and an alternative approach. Brain *130*, e75, author reply e76.

Loomis, A.L., Harvey, E.N., and Hobart, G. (1935). Further observations on the potential rhythms of the cerebral cortex during sleep. Science *82*, 198–200.

Luo, C., Li, Q., Lai, Y., Xia, Y., Qin, Y., Liao, W., Li, S., Zhou, D., Yao, D., and Gong, Q. (2011). Altered functional connectivity in default mode network in absence epilepsy: a resting-state fMRI study. Hum. Brain Mapp. *32*, 438–449.

Magnin, M., Rey, M., Bastuji, H., Guillemant, P., Mauguière, F., and Garcia-Larrea, L. (2010). Thalamic deactivation at sleep onset precedes that of the cerebral cortex in humans. Proc. Natl. Acad. Sci. USA *107*, 3829–3833.

Maquet, P. (2000). Functional neuroimaging of normal human sleep by positron emission tomography. J. Sleep Res. *9*, 207–231.

Massimini, M., Ferrarelli, F., Huber, R., Esser, S.K., Singh, H., and Tononi, G. (2005). Breakdown of cortical effective connectivity during sleep. Science *309*, 2228–2232.

Mayer, G., Jennum, P., Riemann, D., and Dauvilliers, Y. (2011). Insomnia in central neurologic diseases—occurrence and management. Sleep Med. Rev. *15*, 369–378.

Mueller, S., Wang, D., Fox, M.D., Yeo, B.T., Sepulcre, J., Sabuncu, M.R., Shafee, R., Lu, J., and Liu, H. (2013). Individual variability in functional connectivity architecture of the human brain. Neuron *77*, 586–595.

Murphy, K., Birn, R.M., and Bandettini, P.A. (2013). Resting-state fMRI confounds and cleanup. Neuroimage *80*, 349–359.

Musso, F., Brinkmeyer, J., Mobascher, A., Warbrick, T., and Winterer, G. (2010). Spontaneous brain activity and EEG microstates. A novel EEG/fMRI analysis approach to explore resting-state networks. Neuroimage *52*, 1149–1161.

Olbrich, S., Mulert, C., Karch, S., Trenner, M., Leicht, G., Pogarell, O., and Hegerl, U. (2009). EEG-vigilance and BOLD effect during simultaneous EEG/fMRI measurement. Neuroimage *45*, 319–332.

Pereira, F.R., Alessio, A., Sercheli, M.S., Pedro, T., Bilevicius, E., Rondina, J.M., Ozelo, H.F.B., Castellano, G., Covolan, R.J.M., Damasceno, B.P., and Cendes, F. (2010). Asymmetrical hippocampal connectivity in mesial temporal lobe epilepsy: evidence from resting state fMRI. BMC Neurosci. *11*, 66.

Picchioni, D., Duyn, J.H., and Horovitz, S.G. (2013). Sleep and the functional connectome. Neuroimage *80*, 387–396.

Portas, C.M., Krakow, K., Allen, P., Josephs, O., Armony, J.L., and Frith, C.D. (2000). Auditory processing across the sleep-wake cycle: simultaneous EEG and fMRI monitoring in humans. Neuron *28*, 991–999.

Raichle, M.E. (2006). Neuroscience. The brain's dark energy. Science *314*, 1249–1250.

Raichle, M.E., and Snyder, A.Z. (2007). A default mode of brain function: a brief history of an evolving idea. Neuroimage *37*, 1083–1090, discussion 1097–1099.

Richiardi, J., Eryilmaz, H., Schwartz, S., Vuilleumier, P., and Van De Ville, D. (2011). Decoding brain states from fMRI connectivity graphs. Neuroimage *56*, 616–626.

Richter, S., Marsalek, K., Glatz, C., and Gundel, A. (2005). Task-dependent differences in subjective fatigue scores. J. Sleep Res. *14*, 393–400.

Rombouts, S.A., Barkhof, F., Goekoop, R., Stam, C.J., and Scheltens, P. (2005). Altered resting state networks in mild cognitive impairment and mild Alzheimer's disease: an fMRI study. Hum. Brain Mapp. *26*, 231–239.

Roth, B. (1961). The clinical and theoretical importance of EEG rhythms corresponding to states of lowered vigilance. Electroencephalogr. Clin. Neurophysiol. *13*, 395–399.

Sämann, P.G., Wehrle, R., Hoehn, D., Spoormaker, V.I., Peters, H., Tully, C., Holsboer, F., and Czisch, M. (2011). Development of the brain's default mode network from wakefulness to slow wave sleep. Cereb. Cortex *21*, 2082–2093.

Sateia, M.J., Greenough, G., and Nowell, P. (2000). Sleep in neuropsychiatric disorders. Semin. Clin. Neuropsychiatry *5*, 227–237.

Shmueli, K., van Gelderen, P., de Zwart, J.A., Horovitz, S.G., Fukunaga, M., Jansma, J.M., and Duyn, J.H. (2007). Low-frequency fluctuations in the cardiac rate as a source of variance in the resting-state fMRI BOLD signal. Neuroimage *38*, 306–320.

Smith, S.M., Fox, P.T., Miller, K.L., Glahn, D.C., Fox, P.M., Mackay, C.E., Filippini, N., Watkins, K.E., Toro, R., Laird, A.R., and Beckmann, C.F. (2009). Correspondence of the brain's functional architecture during activation and rest. Proc. Natl. Acad. Sci. USA *106*, 13040–13045.

Sorg, C., Riedl, V., Mühlau, M., Calhoun, V.D., Eichele, T., Läer, L., Drzezga, A., Förstl, H., Kurz, A., Zimmer, C., and Wohlschläger, A.M. (2007). Selective changes of resting-state networks in individuals at risk for Alzheimer's disease. Proc. Natl. Acad. Sci. USA *104*, 18760–18765.

Spoormaker, V.I., Schröter, M.S., Gleiser, P.M., Andrade, K.C., Dresler, M., Wehrle, R., Sämann, P.G., and Czisch, M. (2010). Development of a large-scale functional brain network during human non-rapid eye movement sleep. J. Neurosci. *30*, 11379–11387.

Sporns, O. (2012). From simple graphs to the connectome: networks in neuroimaging. Neuroimage *62*, 881–886.

Stern, J.M., Caporro, M., Haneef, Z., Yeh, H.J., Buttinelli, C., Lenartowicz, A., Mumford, J.A., Parvizi, J., and Poldrack, R.A. (2011). Functional imaging of sleep vertex sharp transients. Clin. Neurophysiol. *122*, 1382–1386.

Tagliazucchi, E., von Wegner, F., Morzelewski, A., Borisov, S., Jahnke, K., and Laufs, H. (2012a). Automatic sleep staging using fMRI functional connectivity data. Neuroimage *63*, 63–72.

Tagliazucchi, E., von Wegner, F., Morzelewski, A., Brodbeck, V., and Laufs, H. (2012b). Dynamic BOLD functional connectivity in humans and its electrophysiological correlates. Front. Hum. Neurosci. *6*, 339.

Tagliazucchi, E., von Wegner, F., Morzelewski, A., Brodbeck, V., Borisov, S., Jahnke, K., and Laufs, H. (2013a). Large-scale brain functional modularity is reflected in slow electroencephalographic rhythms across the human non-rapid eye movement sleep cycle. Neuroimage *70*, 327–339.

Tagliazucchi, E., von Wegner, F., Morzelewski, A., Brodbeck, V., Jahnke, K., and Laufs, H. (2013b). Breakdown of long-range temporal dependence in default mode and attention networks during deep sleep. Proc. Natl. Acad. Sci. USA *110*, 15419–15424.

The HD-200 Consortium (2012). The ADHD-200 consortium: a model to advance the translational potential of neuroimaging in clinical neuroscience. Front. Syst. Neurosci. *6*, 62.

Tononi, G. (2004). An information integration theory of consciousness. BMC Neurosci. *5*, 42.

Tzourio-Mazoyer, N., Landeau, B., Papathanassiou, D., Crivello, F., Etard, O., Delcroix, N., Mazoyer, B., and Joliot, M. (2002). Automated anatomical labeling of activations in SPM using a macroscopic anatomical parcellation of the MNI MRI single-subject brain. Neuroimage *15*, 273–289.

Uddin, L.Q., Kelly, A.M., Biswal, B.B., Margulies, D.S., Shehzad, Z., Shaw, D., Ghaffari, M., Rotrosen, J., Adler, L.A., Castellanos, F.X., and Milham, M.P. (2008). Network homogeneity reveals decreased integrity of default-mode network in ADHD. J. Neurosci. Methods *169*, 249–254.

Van de Ville, D., Britz, J., and Michel, C.M. (2010). EEG microstate sequences in healthy humans at rest reveal scale-free dynamics. Proc. Natl. Acad. Sci. USA *107*, 18179–18184.

Van Dijk, K.R., Sabuncu, M.R., and Buckner, R.L. (2012). The influence of head motion on intrinsic functional connectivity MRI. Neuroimage *59*, 431–438.

Van Essen, D.C., and Ugurbil, K. (2012). The future of the human connectome. Neuroimage *62*, 1299–1310.

Vanhaudenhuyse, A., Noirhomme, Q., Tshibanda, L.J.F., Bruno, M.A., Boveroux, P., Schnakers, C., Soddu, A., Perlbarg, V., Ledoux, D., Brichant, J.F., Moonen, G., et al. (2010). Default network connectivity reflects the level of consciousness in non-communicative brain-damaged patients. Brain *133*, 161–171.

Vincent, J.L., Patel, G.H., Fox, M.D., Snyder, A.Z., Baker, J.T., Van Essen, D.C., Zempel, J.M., Snyder, L.H., Corbetta, M., and Raichle, M.E. (2007). Intrinsic functional architecture in the anaesthetized monkey brain. Nature *447*, 83–86.

Wang, L., Zang, Y., He, Y., Liang, M., Zhang, X., Tian, L., Wu, T., Jiang, T., and Li, K. (2006). Changes in hippocampal connectivity in the early stages of Alzheimer's disease: evidence from resting state fMRI. Neuroimage *31*, 496–504.

Zang, Y.F., He, Y., Zhu, C.Z., Cao, Q.J., Sui, M.Q., Liang, M., Tian, L.X., Jiang, T.Z., and Wang, Y.F. (2007). Altered baseline brain activity in children with ADHD revealed by resting-state functional MRI. Brain Dev. *29*, 83–91.

Zhang, D., and Raichle, M.E. (2010). Disease and the brain's dark energy. Nat. Rev. Neurol. *6*, 15–28.

Zhou, Y., Liang, M., Tian, L., Wang, K., Hao, Y., Liu, H., Liu, Z., and Jiang, T. (2007). Functional disintegration in paranoid schizophrenia using resting-state fMRI. Schizophr. Res. *97*, 194–205.